The method of images revisited: Approximate solutions in wedge-shaped aquifers of arbitrary angle

I.A. Nikoletos[1*], K.L. Katsifarakis[1]

[1]Division of Hydraulics and Environmental Engineering,

Dept. of Civil Engineering, A.U.Th,

GR- 54124 Thessaloniki, Greece

[*] Corresponding author: e-mail: irakniko@civil.auth.gr

Abstract

This paper focuses on deriving new approximate analytical solutions in wedge-shaped aquifers. The proposed methodology is applicable to any type of aquifer namely, leaky, confined and unconfined, under both steady state and transient flow conditions. By applying the method of images and seperating the flow field into sections using physical arguements, analytical expressions are obtained for the drawdown function. In contrast to the conventional theory, the proposed solutions are applicable to arbitrary wedge angle. Comparison of the results of the derived approximate analytical solutions to numerical ones, is considered necessary to ensure its validity. MODFLOW, a well-known numerical tool is used to calculate the numerical results. The results indicate that the boundary conditions are fully observed, the drawdown is feasible to be calculated at any point of the real flow field (continuity of the drawdown function) and discrepancies compared to numerical results are considered negligible. The main advantage of

the proposed procedure is that it can be easily used in conjunction with meta-heuristic algorithms to solve groundwater resources optimization problems.

Keywords

Wedge-shaped aquifers; method of images; groundwater flow; approximate analytical solutions; MODFLOW; Well function

1. Introduction

Aquifers bounded by two boundaries, constant head such as streams and lakes or no flux, such as impermeable rocks, intersecting at angle smaller than 90^o are called wedge-shaped (Mahdavi, 2021). Their study has been the subject of research interest over the years. Most of the research papers were focused on analytical, approximate analytical and semi-analytical expressions for drawdown calculation and estimation of the aquifer's parameters (Singh, 2001; Yeh et. al., 2008).

Analytical procedures have been followed in several research papers to obtain expressions for the drawdown function. The well-known Hankel transform has been used by Chan et. al. (1978), Yeh et. al. (2006) and Chuang and Yeh (2018) to obtain analytical solutions in wedge-shaped aquifers under steady state and transient flow conditions respectively. Chen et. al. (2009) have applied the method of images to describe the aquifer's response to a constant pumping well. Other methods used to derive analytical solutions to wedge-shaped aquifers are the revisited Strack-Chernysov model (Kacimov et.al., 2016), fractional calculus (Kavvas et. al., 2017) and Laplace transform (Lin et. al., 2018). Recently, more complicated aquifer's shapes, such as

triangle-shaped, annular wedge-shaped, trapezoidal-shaped, have been studied analytically (Asadi-Aghbolaghi & Seyyedian, 2010; Kacimov et. al., 2017; Leray et. al., 2019; Mahdavi, 2019; Mahdavi and Yazdani, 2021; Mahdavi, 2022; Nagheli et. al., 2020; Zlotnik et. al., 2015).

When no analytical solutions are available, semi-analytical and approximate analytical methods have been adopted to investigate wedge-shaped aquifers. Dimensionless type curves of flux-time and drawdown-time are given for homogeneous aquifers by Sedghi et. al. (2010) and Sedghi et. al. (2012) as well as for heterogeneous ones from Samani and Sedghi (2015), using integrals transform methods. Wang et al. (2018) presented a Laplace transform boundary element method to simulate the groundwater flow. Estimation of hydraulic parameters and prediction of the discharge of qanat in alluvial aquifers is achieved via the semi-analytical approach introduced by Sedghi and Zhan (2022). On the other hand, approximate analytical solutions are simplified expressions aiming to describe complex problems with good accuracy. Approximate solutions to Forcheimer equation (Moutsopoulos & Tsihrintzis, 2005; Okuyade et. al., 2022)) and groundwater response to tidal fluctuations (Monachesi & Guarracino, 2011) are only a few examples showing their usefulness. Expressions obtained from approximate procedures suit perfectly to be used in combination with meta-heuristic methods (Christelis et. al., 2019; Karpouzos & Katsifarakis 2021; Mallios et. al., 2022; Rodriguez-Pretelin & Nowak 2019). Further discussion about approximate analytical solutions will follow in section 3.

In this framework, approximate analytical solutions for wedge-shaped aquifers are sought. Observance of boundary conditions, either constant head or no flux, as well as continuity of the drawdown function were set as prerequisites. The concept of the proposed methodology is the division of the real flow field into two sections, where different fictitious wells are taken into

account. The method of images has been applied to introduce the fictitious, pumping or injection wells.

2. Outline of the method of images

The basic concept of the method of images is that a boundary can be "removed" by adding a number of fictitious (or image) wells, symmetrical of the real ones with respect to it, resulting into an equivalent infinite flow field (Haitjema, 2006; Mahdavi, 2020; Nikoletos, 2020). The sign of the flow rate of each image well depends on the boundary condition and guarantees its observance (Katsifarakis et al., 2018; Samani & Zarei-Doudeji, 2012). From mathematical point of view, it is a specific application of the Green's function and is applicable to problems described by the Poisson equation (Mohamed & Paleologos, 2018). Its use is extensive in many scientific fields such as groundwater hydraulics (Kuo et. al., 1994), electrostatics (Nguyen & Mehrabian, 2021), magnetics (Curtis et. al., 2015) and optics. The method of images has been widely used in groundwater flow simulation problems to calculate hydraulic head level drawdown (Atangana, 2014; Nikoletos & Katsifarakis, 2022; Penny et. al., 2020), to describe interaction between ground and surface water (Anderson, 2003) and to optimize the management of aquifers (Katsifarakis, 2008) and especially coastal aquifers facing saltwater intrusion problems (Etsias et. al., 2021; Mantoglou, 2003). It is worth mentioning that the method of images gives exact solutions in wedge-shaped aquifers bounded by two boundaries intersecting at angles of : 90^o, 60^o, 45^o, 30^o etc. (each angle verifying eq. 1)

$$\theta = \frac{360^\circ}{N+1},\ N = 3, 5, 7, \ldots \quad (1)$$

Where θ, is the boundary intersection angle and N, the number of fictitious wells.

3. Approximate analytical solutions

3.1 Previous Studies

Due to the complexity of many flow fields, exact solutions cannot be found. In such cases, approximate analytical solutions could be a good alternative, if the introduced error is acceptable and the computational volume low. On the other hand, solutions produced by numerical methods are inherently approximate, too. Convergence of both approximate analytical and numerical methods point out the validity of the proposed solutions.

In the following paragraphs, the usefulness of approximate analytical solutions to groundwater resources management problems is presented. Drawdown distribution in semi-infinite aquifers is easily calculated via approximate solutions (Nikoletos & Katsifarakis, 2022; Sun et. al., 2011; Zlotnik et. al., 2017; Yang et. al., 2014). Accurate calculation of stream depletion rate due to pumping wells located at adjacent aquifers is another scientific issue where approximate solutions have been a valuable asset (Huang & Yeh, 2015; Huang et. al., 2018; Lapides et. al., 2022; Smerdon et. al., 2012 ; Teloglou & Bansal, 2012; Zipper et al., 2019). Their combination with heuristic methods to groundwater optimization problems reveal the ability to keep the computational load much smaller in comparison with numerical ones (Christelis & Mantoglou, 2019).

3.2 Basic concept of the proposed solutions

The aim of the proposed solutions is to calculate with good accuracy the drawdown distribution in a wedge-shaped flow field, while observing the boundary conditions. Following the approach developed by Nikoletos and Katsifarakis (2022), we divided the real flow field into two sections. In each section a number of fictitious wells are used in a way that observance of the boundary conditions is achieved. The proposed division of the flow field in two sections, does not disrupt continuity of the drawdown, but the flow velocity field is discontinuous, along the straight line that separates the field.

The accuracy of the results as well as the applicability range of the proposed approximate solutions are discussed in the following sections.

3.3 Comparison with previous studies

Kuo et. al. (1994) proposed a new approach for predicting drawdown in aquifer with irregularly shaped boundaries using the image well method. More recently, a novel methodology for estimation of stream filtration from a meandering stream, is introduced by Huang and Yeh (2015) by applying image well theory. In both papers the decision variables were the flow rates of the image wells which are determined by solving a system of equations. In this paper the decision variables are the number of fictitious wells taking into account the physical interpretation of the method. The proposed methodology is more suitable to problems where the intersecting boundaries are straight lines while the aforementioned methods are preferred where the boundaries are curved. It is worth mentioning that combination of the method proposed by Nikoletos and Katsifarakis with the method introduced by Kuo et. al. (1994) or Huang and Yeh (2015) could lead to more accurate results for the calculation of the drawdown. This will be an issue of future study.

3.4 Structure of the drawdown function

The proposed methodology can be applied to any type of aquifer under steady state and transient flow conditions. The drawdown functions at any point (*x,y*), due to pumping from a single well, in confined, unconfined and leaky aquifersare given by the following relationships respectively (Theim, 1906):

$$s(x,y) = -\frac{1}{2\pi T} Q_w \ln \frac{\sqrt{(x-x_w)^2+(y-y_w)^2}}{R} \quad (2.a)$$

$$s(x,y) = \frac{1}{2\pi T} Q_w K_o\left(\frac{\sqrt{(x-x_w)^2+(y-y_w)^2}}{L}\right) \quad (2.b)$$

$$H^2 = H_1^2 + \frac{1}{\pi K} Q_w \ln \frac{\sqrt{(x-x_w)^2+(y-y_w)^2}}{R} \quad (2.c)$$

Where, Q_w is the flow rate of the well, (x_w, y_w) are the well's coordinates, *K* is the hydraulic conductivity, *T* is the aquifer's transmissivity, *R* is the radius of influence, *L* is the leaky coefficient, K_o is the modified Bessel function of second kind and zero order and *H* and H_1 are the distances between water table and initial water table and a reference level.

To demonstrate the procedure, we consider steady flow in confined aquifers.

3.4.1 Intersecting angle – Case of $90^o < \theta < 60^o$

In the following paragraphs, we present solutions for wedge-shaped aquifers where the boundaries are both of constant head or impermeable. We demonstrate the proposed methodology for constant head boundaries. The process is the same in case of impermeable boundaries, except the kind of the fictitious wells.

The exact solution for the drawdown due to a pumping well in flow fields bounded by two boundaries intersecting at angle 90^o and 60^o makes use of 3 and 5 fictitious wells, respectively.

Based on that, we postulate that the proposed solutions should make use of 3 to 5 fictitious wells. As shown in Fig. 3, W_{i-1} and W_{i-2} are the images of the real well with respect to the closest and the furthest boundary respectively; we call them first-order images. W_{i-3} and W_{i-4} are the images of W_{i-1} and W_{i-2} with respect to the other boundary; we call them second-order images. W_{i-5} and W_{i-6}, resulting in a similar way, are the third-order images, and so on. The odd order images of a pumped well are injection wells, while the even order ones represent pumping wells.

From the physical point of view, the influence of the image wells should decrease, as their order increases. For instance, the first order images should affect more the conditions in the real flow field, namely they should be located closer to it than the second order ones, the second order images should be closer to the real flow field than the third order ones and so on. The largest order image wells should operate alternately in parts of the flow field, in order to satisfy the boundary conditions. According to the geometrical proof found in Appendix A, if the angle θ is larger than 72^o, the third order images are closer to the real flow field than the second order ones. Consequently, we conclude that for angles larger than 72^o, 3 fictitious wells should be used, while for angles smaller than 72^o, 5 fictitious wells should be used, provided that the conditions described by inequalities (8) and (9) of Appendix A are also satisfied. Otherwise the largest order images should not be used.

From the physical point of view, we expect that the drawdown at any point of the real flow field decreases as the angle between the boundaries decreases. According to Fig. 1, by isolating W_r and W_{i-1} results into conditions equal to one constant head boundary. The second constant head boundary should further reduce the drawdown. Therefore the system of W_{i-2}, W_{i-3}, W_{i-4} and W_{i-5} or W_{i-6} (for the respective system of W_r and W_{i-2}) should represent the influence of the second boundary. This reduction depends on the distance of the above mentioned system from the real

flow field. As the angle θ increases, the system of the image wells diverges from the real flow field, so its influence decreases, too.

Fig. 1. Seperation of the wells into two groups. *Note*: BC stands for boundary condition.

Therefore, the following two-branch functions could describe the drawdown distribution to the real flow field in each case.

For $90^o > \theta > 72^o$

$$s(x,y) = \begin{cases} -\frac{1}{2\pi T} Q_w \ln \frac{\sqrt{(x-x_w)^2+(y-y_w)^2}\sqrt{(x-x_{w4})^2+(y-y_{w4})^2}}{\sqrt{(x-x_{w1})^2+(y-y_{w1})^2}\sqrt{(x-x_{w2})^2+(y-y_{w2})^2}} \\ -\frac{1}{2\pi T} Q_w \ln \frac{\sqrt{(x-x_w)^2+(y-y_w)^2}\sqrt{(x-x_{w3})^2+(y-y_{w3})^2}}{\sqrt{(x-x_{w1})^2+(y-y_{w1})^2}\sqrt{(x-x_{w2})^2+(y-y_{w2})^2}} \end{cases} \quad (3)$$

Fig. 2. Wedge-shaped aquifer $90^o > \theta > 72^o$

For $72^o > \theta > 60^o$

$$s(x,y) = \begin{cases} -\frac{1}{2\pi T} Q_w \ln \frac{\sqrt{(x-x_w)^2+(y-y_w)^2}\sqrt{(x-x_{w3})^2+(y-y_{w3})^2}\sqrt{(x-x_{w4})^2+(y-y_{w4})^2}}{\sqrt{(x-x_{w1})^2+(y-y_{w1})^2}\sqrt{(x-x_{w2})^2+(y-y_{w2})^2}\sqrt{(x-x_{w5})^2+(y-y_{w5})^2}} \\ -\frac{1}{2\pi T} Q_w \ln \frac{\sqrt{(x-x_w)^2+(y-y_w)^2}\sqrt{(x-x_{w3})^2+(y-y_{w3})^2}\sqrt{(x-x_{w4})^2+(y-y_{w4})^2}}{\sqrt{(x-x_{w1})^2+(y-y_{w1})^2}\sqrt{(x-x_{w2})^2+(y-y_{w2})^2}\sqrt{(x-x_{w6})^2+(y-y_{w6})^2}} \end{cases} \quad (4)$$

Fig. 3. Wedge-shaped aquifer $72^o > \theta > 51.4^o$

3.4.2 Intersecting angle – Case of $60^o > \theta > 45^o$

If the intersecting angle of the boundaries is 60^o, the exact analytical solution makes use of 5 fictitious wells. If the angle is 45^o, 7 fictitious wells are placed to the equivalent infinite flow

191 field. We postulate, then, that the proposed approximate solutions should make use of 5 to 7
192 fictitious wells. The main difference compared to the case 90^o-60^o is that the largest order images
193 are pumping wells. Taking into account the physical interpretation of the aquifer's response, the
194 4^{th} order images should be located farther than the 3^{rd} order ones from the real flow field.

195 According to the geometrical proof found in Appendix A, if the angle is larger than 51.42^o, the
196 4^{th} order images are closer to the real flow field than the 3^{rd} order ones. The largest order image
197 wells should be used alternately in parts of the flow field, in order to ensure the observance of
198 boundary conditions. Consequently, we conclude that for angles larger than 51.42^o we should use
199 5 fictitious wells, while for angles smaller than 51.42^o, 7 fictitious wells should be used,
200 provided that the conditions described by inequalities (8) and (9) of Appendix A are also
201 satisfied. Otherwise the largest order images should not be used.

202 Verification of the drawdown reduction as the angle θ decreases is needed. We examine
203 seperately W_r and W_{i-1} and rest of the wells. According to Section 3.4.1 the system of wells W_{i-2},
204 W_{i-3}, W_{i-4}, W_{i-5} or W_{i-6} (for the respective system of W_r and W_{i-2}) offers water quantity to the real
205 flow field. Consequently, it 's proved that W_{i-5} and W_{i-6} are closer to the real flow field than W_{i-7}
206 and W_{i-8}, respectively. According to the geometrical proof of Appendix A, the aforementioned
207 conditions holds.

208 Hence, the following two-branch functions describe the drawdown distribution to the real flow
209 field in each case.

210 <u>For $60^o > \theta > 51.42^o$</u>

211
$$s(x,y) = \begin{cases} -\frac{1}{2\pi T} Q_w \ln \frac{\sqrt{(x-x_w)^2+(y-y_w)^2}\sqrt{(x-x_{w3})^2+(y-y_{w3})^2}\sqrt{(x-x_{w4})^2+(y-y_{w4})^2}}{\sqrt{(x-x_{w1})^2+(y-y_{w1})^2}\sqrt{(x-x_{w2})^2+(y-y_{w2})^2}\sqrt{(x-x_{w5})^2+(y-y_{w5})^2}} \\ -\frac{1}{2\pi T} Q_w \ln \frac{\sqrt{(x-x_w)^2+(y-y_w)^2}\sqrt{(x-x_{w3})^2+(y-y_{w3})^2}\sqrt{(x-x_{w4})^2+(y-y_{w4})^2}}{\sqrt{(x-x_{w1})^2+(y-y_{w1})^2}\sqrt{(x-x_{w2})^2+(y-y_{w2})^2}\sqrt{(x-x_{w6})^2+(y-y_{w6})^2}} \end{cases} \quad (5)$$

It is worth mentioning that in this case and the case of $90^o > \theta > 72^o$ the number of fictitious wells coincides.

For $51.42^o > \theta > 45^o$

$$s(x,y) = \begin{cases} -\frac{1}{2\pi T} Q_w \ln \frac{\sqrt{(x-x_w)^2+(y-y_w)^2}\sqrt{(x-x_{w3})^2+(y-y_{w3})^2}\sqrt{(x-x_{w4})^2+(y-y_{w4})^2}\sqrt{(x-x_{w8})^2+(y-y_{w8})^2}}{\sqrt{(x-x_{w1})^2+(y-y_{w1})^2}\sqrt{(x-x_{w2})^2+(y-y_{w2})^2}\sqrt{(x-x_{w5})^2+(y-y_{w5})^2}\sqrt{(x-x_{w6})^2+(y-y_{w6})^2}} \\ -\frac{1}{2\pi T} Q_w \ln \frac{\sqrt{(x-x_w)^2+(y-y_w)^2}\sqrt{(x-x_{w3})^2+(y-y_{w3})^2}\sqrt{(x-x_{w4})^2+(y-y_{w4})^2}\sqrt{(x-x_{w7})^2+(y-y_{w7})^2}}{\sqrt{(x-x_{w1})^2+(y-y_{w1})^2}\sqrt{(x-x_{w2})^2+(y-y_{w2})^2}\sqrt{(x-x_{w5})^2+(y-y_{w5})^2}\sqrt{(x-x_{w6})^2+(y-y_{w6})^2}} \end{cases} \quad (6)$$

Fig. 4. Wedge-shaped aquifer $51.4^o > \theta > 45^o$

3.4.3 Intersecting angle – Cases of $\theta < 45^o$

For the rest of the cases, we follow exactly the same methodology as described in sections 3.4.1 and 3.4.2, for consecutive analytical solutions. The determination of the critical angle of each case as well as the operating wells of each section are based on eq. 11 and Fig. 6, found in Appendix A.

4. Evaluation through comparison with numerical simulation results

MODFLOW (Harbaugh, 2005; Harbaugh et. al., 2017), an established, finite-difference, groundwater flow simulation model is used for numerical evaluation of the proposed solutions. It is widely used by hydrogeologists to simulate real and theoretical flow fields for estimation of the response of the aquifers (Malekzadeh et. al., 2019). The program has been applied

229 extensively to aquifers bounded by two or more irregular shaped boundaries (Aghlmand and
230 Abbasi, 2019; Karimi et. al., 2019).

231

232 Here we use MODFLOW to evaluate the quality of the proposed approximate solutions. We
233 consider 6 cases of wedge-shaped aquifers, bounded by two constant head boundaries,
234 intersecting at the point O (0, 2000). One boundary is described by the equation x = 0. A well
235 with coordinates (320, 1500) pumps at a flow rate Q_W = 0.02 m^3/s. The hydraulic parameters of
236 the well and the aquifer are listed below.

237 a) Radius of the well r_0 = 0.5 m

238 b) Hydraulic Conductivity K = 0.0000016 m/s

239 c) Thickness of aquifer a = 100 m

240 We consider steady-state flow conditions to facilitate the comparison with the approximate
241 analytical solutions.

242 A grid of 5 x 5 m has been used to run MODFLOW and the results have been compared to those
243 obtained from the approximate analytical solutions. Visualization of the results has been made
244 through ModelMuse (Winston, 2009; Winston, 2020), a well-known graphical user interface for
245 groundwater simulation models. The results for 6 θ values are discussed in the following
246 paragraphs.

247 For $\theta=90^o$, 60^o and 45^o the solutions are exact. These cases serve rather to check MODFLOW
248 results. The analytical solutions give slightly larger values than MODFLOW. Discrepancies are
249 smaller than 5% at all points of the real flow field except the location of the well.

For $\theta=80^o$, 65^o and 55^o the solutions are approximate. The approximate analytical solutions render larger drawdown values than MODFLOW. Discrepancies are smaller than 6% at all points of the real flow field except the location of the well.

Equipotential lines, obtained by the two methods, are shown in Fig. 5

Fig. 5. Equipotential lines for different boundary intersction angles obtained by approximate solution and MODFLOW

5. Conclusions and Discussion

New functions for the calculation of the drawdown distribution of wedge-shaped aquifers via approximate analytical procedures are presented, based on the method of images. Observance of the boundary conditions is achieved through the use of two-branch functions. The largest order fictitious wells are activated alternately in parts of the flow field. The division of the flow field in two sections does not disrupt continuity of the drawdown. The only drawback is that the flow velocity field is discontinuous, along the straight line that separates the field.

To check the validity of the approximate solutions, results for six application examples have been compared to numerical ones, obtained by MODFLOW. For θ equal to 90^o, 60^o and 45^o, namely when the method of images is exact, the discrepancies are generally smaller than 5%, while in the other cases, discrepancies are generally smaller than 6%. The main advantage of the proposed solutions is that the respective computational load is low, so they can be easily used in conjunction with meta-heuristic algorithms to solve groundwater resources optimization problems.

Open Research Section

Data Availability Statement

The paper is purely theoretical. Data were not used, nor created for this research.

Software Availability Statement

Software for this research is available through https://zenodo.org/record/7501194

Appendix A: Geometrical Proof

Let angle θ be between two consecutive angles, namely θ_k and θ_{k-2} where the image well method is exact and the number of fictitious wells is k and k-2 respectively.

Let a and b be the angles of OW_r with the field boundaries Ox_1 and Ox_2 respectively.

Let angle c be given by the following equation:

$$(\frac{k+(k-2)}{4})\theta + c = 180^o \Rightarrow c = 180^o - (\frac{k+(k-2)}{4})\theta \quad (7)$$

If the angle $\theta = (Ox_1, Ox_2) < \frac{360^o}{k}$, the penultimate order image $W_{i-(k-2)}$ is closer than the last-order image W_{i-k} to W_r and to any point of the real field.

Proof: If $b < c$, then $(Ox_2, W_{i-2}) < c$, namely W_{i-2} lies on the same side of Ox_n, with W_r. Consequently, W_{i-4}, the image well of W_{i-2} with respect to Ox_1 lies under the side of Ox_{n+1}. Since Ox_2 is the bisector of Ox_1' and Ox_{n+1}', the image well of W_{i-4} with respect to Ox_2, namely W_{i-6}, lies on the opposite site of Ox_1. The same condition holds for the consecutive mirror wells with respect to the corresponding boundary until the penultimate well, namely $W_{i-(k-2)}$. For the last order image well, Ox_1 is the perpendicular bisector of $W_{i-(k-2)}$ and W_{i-k}. Therefore $W_{i-(k-2)}$ and W_{i-k} lie on the opposite site of Ox_1. As shown in Fig. 6 the following relationships hold:

$$b < c \quad (8)$$

293 $a < c$

294 (9)

295 Also, we take advantage of the following property

296 $$a + b = \theta \Rightarrow b = \theta - a \qquad (10)$$

297 Adding up the inequalities (8) and (9) resulting

$$a + b < 2c \xrightarrow[(7)-(10)]{} \theta < 2\left(180^o - \left(\frac{k + (k-2)}{4}\right)\theta\right) \Rightarrow \theta < 360^o - (k-1)\theta \Rightarrow k\theta < 360^o$$

298 $$\Rightarrow \quad \theta < \frac{360^o}{k}$$

299 (11)

300 **Fig. 6.** Geometrical relationships between real and fictitious wells for arbitrary wedge angle.

301

302 **References**

303

304 1. Aghlmand, R. and Abbasi, A. (2019) "Application of MODFLOW with Boundary
305 Conditions Analyses Based on Limited Available Observations: A Case Study of Birjand
306 Plain in East Iran". **Water,** 11(9), https://doi.org/10.3390/w11091904
307 2. Anderson, E.I. (2003) "An analytical solution representing groundwater–surface water
308 interaction". **Water Resources Research,** 39(3), https://doi.org/10.1029/2002WR001536
309 3. Asadi-Aghbolaghi, M. and Seyyedian, H. (2010) "An analytical solution for groundwater
310 flow to a vertical well in a triangle-shaped aquifer". **Journal of Hydrology,** 393(3-4):341-
311 348, https://doi.org/10.1016/j.jhydrol.2010.08.034

4. Atangana, A. (2014) “Drawdown in prolate spheroidal–spherical coordinates obtained via Green’s function and perturbation methods”. **Communications in Nonlinear Science and Numerical Simulation,** 19(5):1259-1269, https://doi.org/10.1016/j.cnsns.2013.09.031
5. Chan, Y.K., Mullineaux, N., Reed, J.R. and Wells, G.G. (1978) “Analytic solutions for drawdowns in wedge-shaped artesian aquifers”. **Journal of Hydrology,** 36(3-4):233-246, https://doi.org/10.1016/0022-1694(78)90146-4
6. Chen, Y.J., Yeh, H.D. and Yang, S.Y. (2009) “Analytical Solutions for Constant-Flux and Constant-Head Tests at a Finite-Diameter Well in a Wedge-Shaped Aquifer”. **Journal of Hydrologic Engineering,** 135(4), https://doi.org/10.1061/(ASCE)0733-9429(2009)135:4(333)
7. Christelis, V., Kopsiaftis, G. and Mantoglou, A. (2019) “Performance comparison of multiple and single surrogate models for pumping optimization of coastal aquifers”, **Hydrological Sciences Journal**, 64(3) https://doi.org/10.1080/02626667.2019.1584400
8. Christelis, V. and Mantoglou, A. (2019) “Pumping Optimization of Coastal Aquifers Using Seawater Intrusion Models of Variable-Fidelity and Evolutionary Algorithms”. **Water Resources Management,** 33:555-568, https://doi.org/10.1007/s11269-018-2116-0
9. Chuang, M.H. and Yeh, H.D. (2018) “An Analytical Solution of Groundwater Flow in Wedge-shaped Aquifers with Estuarine Boundary Conditions.”. **Water Resources Management,** 32:5027-5039, https://doi.org/10.1007/s11269-018-2125-z
10. Curtis, M., Paulides, J.H. and Lomonova, E.A. (2015) “An overview of analytical methods for magnetic field computation”. **Tenth International Conference on Ecological Vehicles and Renewable Energies (EVER),** 10.1109/EVER.2015.7112938

11. Etsias, G., Hamill, G.A., Aguila, J.F., Benner, E.M., McDonnell, M.C., Ahmed, A.A. and Flynn, R. (2021) "The impact of aquifer stratification on saltwater intrusion characteristics. Comprehensive laboratory and numerical study". **Hydrological Processes,** 35(4):14120, https://doi.org/10.1002/hyp.14120
12. Haitjema, H. (2006) "The Role of Hand Calculations in Ground Water Flow Modeling". **Journal of Hydrology,** 36(3-4):233-246, https://doi.org/10.1111/j.1745-6584.2006.00189.x
13. Harbaugh, A.W., (2005) "MODFLOW-2005, the U.S. Geological Survey modular ground-water-model- the Ground Water Flow Process: U.S. Geological Survey Techniques and Methods 6-A16
14. Harbaugh, A.W., Langevin, C.D., Hughes, J.D., Niswonger, R.N. and Konikow, L.F. (2017) "MODFLOW-2005 version 1.12.00, the U.S. Geological Survey modular groundwater model". U.S. Geological Survey Software Release, 03 February 2017, http://dx.doi.org/10.5066/F7RF5S7G
15. Huang, C.S. and Yeh, H.D. (2015) "Estimating stream filtration from a meandering stream under the Robin condition". **Water Resources Research**, 51, 4848-4857, https://doi.org/10.1002/2015WR016975
16. Huang, C.S., Yang, T. and Reed, Yeh, H.D. (2018) "Review of analytical models to stream depletion induced by pumping: Guide to model selection". **Journal of Hydrology,** 561:277-285, https://doi.org/10.1016/j.jhydrol.2018.04.015
17. Kacimov, A.R., Kayumov, I.R. and Al-Maktoumi, A. (2016) "Rainfall induced groundwater mound in wedge-shaped promontories: The Strack–Chernyshov model revisited". **Advances in Water Resources,** 97:110-119, https://doi.org/10.1016/j.advwatres.2016.08.011

18. Kacimov, A.R., Maklakov, D.V. and Kayumov, I.R.. (2017) “Free Surface Flow in a Microfluidic Corner and in an Unconfined Aquifer with Accretion: The Signorini and Saint-Venant Analytical Techniques Revisited”. **Transport in Porous Media,** 116:115-142, https://doi.org/10.1007/s11242-016-0767-y
19. Karimi, L., Motagh, T. and Entezam, I. (2019) “Modeling groundwater level fluctuations in Tehran aquifer: Results from a 3D unconfined aquifer model”. **Groundwater for Sustainable Development,** 8:439-449, https://doi.org/10.1016/j.gsd.2019.01.003
20. Karpouzos, D.K. and Katsifarakis, K.L. (2021) “A new benchmark optimization problem of adaptable difficulty: theoretical considerations and practical testing”. **Operational Research,** 21:231-250, https://doi.org/10.1007/s12351-019-00462-8
21. Katsifarakis, K.L. (2008) “Groundwater pumping cost minimization-An analytical approach”. **Water Resources Management,** 22(8):1089-1099, https://doi.org/10.1007/s11269-007-9212-x
22. Katsifarakis, K.L., Nikoletos, I.A. and Stavridis, C. (2018) “Minimization of Transient Groundwater Pumping Cost - Analytical and Practical Solutions”. **Water Resources Management,** 32:1053-1069, https://doi.org/10.1007/s11269-017-1854-8
23. Kavvas, M.L., Tu, T., Ercan, A. and Polsinelli, J. (2017) “Fractional governing equations of transient groundwater flow in confined aquifers with multi-fractional dimensions in fractional time”. **Earth System Dynamics,** 8:921-929, https://doi.org/10.5194/esd-8-921-2017
24. Kuo, M.C.T., Wang, W.L., Lin, D.S. and Chiang, C.J. (1994) “An Image-Well Method for Predicting Drawdown Distribution in Aquifers with Irregularly Shaped Boundaries”. **Groundwater** Vol. 32(5), 794-804, https://doi.org/10.1111/j.1745-6584.1994.tb00921.x

25. Lapides, D.A., Maitland, B.M., Zipper, S.C., Latzka, A.W., Pruitt, A. and Greve, R. (2022) "Advancing environmental flows approaches to streamflow depletion management". **Journal of Hydrology,** 607:127447, https://doi.org/10.1016/j.jhydrol.2022.127447
26. Leray, S., Gauvain, A. and Dreuzy, J.R. (2019) "Residence time distributions in non-uniform aquifer recharge and thickness conditions – An analytical approach based on the assumption of Dupuit-Forchheimer". **Journal of Hydrology,** 574:110-128, https://doi.org/10.1016/j.jhydrol.2019.04.032
27. Lin, C.C., Chang, Y.C. and Yeh, H.D. (2018) "Analysis of groundwater flow and stream depletion in L-shaped fluvial aquifers". **Hydrology and Earth System Sciences,** 22(4):2359-2375, https://doi.org/10.5194/hess-22-2359-2018
28. Mahdavi, A. (2019) "Transient-state Analytical Solution for Arbitrarily-Located Multiwells in Triangular-Shaped Unconfined Aquifer". **Water Resources Management,** 33:3615-3631, https://doi.org/10.1007/s11269-019-02324-6
29. Mahdavi, A. (2020) "Steady-state response of annular wedge-shaped aquifers to arbitrarily-located multiwells with regional flow". **Journal of Hydrology,** 147:103823, https://doi.org/10.1016/j.jhydrol.2020.124906
30. Mahdavi, A. (2021) "Response of dual-zone heterogeneous wedge-shaped aquifers under steady-state pumping and regional flow". **Advances in Water Resources,** 147:103823, https://doi.org/10.1016/j.advwatres.2020.103823
31. Mahdavi, A. (2022) "Well hydraulics in dual-zone heterogeneous wedge-shaped aquifers under an ambient flow from stream-wise varying boundary heads". **Journal of Hydrology,** 612 (A):128063, https://doi.org/10.1016/j.jhydrol.2022.128063

32. Mahdavi, A. and Yazdani, (2021) “A novel analytical solution for warping analysis of arbitrary annular wedge-shaped bars”. **Archive of Applied Mechanics,** 91:1247-1255, https://doi.org/10.1007/s00419-020-01858-1
33. Malekzadeh, M., Kardar, S. and Shabanlou, S. (2019) “Simulation of groundwater level using MODFLOW, extreme learning machine and Wavelet-Extreme Learning Machine models”, **Groundwater for Sustainable Development,** 9, https://doi.org/10.1016/j.gsd.2019.100279
34. Mallios, Z., Siarkos, I., Karagiannopoulos, P. and Tsiarapas, A. (2022) “Pumping energy consumption minimization through simulation-optimization modelling”, **Journal of Hydrology,** 612(A):128062, https://doi.org/10.1016/j.jhydrol.2022.128062
35. Mantoglou, A. (2003) “Pumping management of coastal aquifers using analytical models of saltwater intrusion”. **Water Resources Research,** 39(12), https://doi.org/10.1029/2002WR001891
36. Mohamed, A.M. and Paleologos, E.K. (2018) “Groundwater”. **Fundamentals of Environmental Engineering,** https://doi.org/10.1016/B978-0-12-804830-6.00005-3
37. Monachesi, L.B. and Guarracino, L. (2011) “Exact and approximate analytical solutions of groundwater response to tidal fluctuations in a theoretical inhomogeneous coastal confined aquifer”. **Hydrogeology Journal,** 19:1443-1449, https://doi.org/10.1007/s10040-011-0761-y
38. Moutsopoulos, K.N. and Tsihrintzis, V.A. (2005) “Approximate analytical solutions of the Forchheimer equation”. **Journal of Hydrology,** 309(1-4):93-103, https://doi.org/10.1016/j.jhydrol.2004.11.014

39. Nagheli, S., Samani, N. and Barry, D.A. (2020) “Capture zone models of a multi-well system in aquifers bounded with regular and irregular inflow boundaries”. **Journal of Hydrology X,** 7:100053, https://doi.org/10.1016/j.hydroa.2020.100053
40. Nguyen, K. and Mehrabian, A. (2021) “Capture zone models of a multi-well system in aquifers bounded with regular and irregular inflow boundaries”. **Physical Mesomechanics,** 24:20-31, https://doi.org/10.1134/S1029959921010045
41. Nikoletos, I.A. (2020) “Analytical Solutions of Intermittent Transient Groundwater Pumping Cost”. **Journal of Hazardous Toxic and Radioactive Waste,** 24(4), https://doi.org/10.1061/(ASCE)HZ.2153-5515.0000544
42. Nikoletos, I.A. and Katsifarakis, K.L. (2022) “Approximate application of the method of images in fields with two boundaries intersected at angles between 180° and 90°”. **Journal of Hydrology,** 607:127519, https://doi.org/10.1016/j.jhydrol.2022.127519
43. Okuyade, W.I., Abbey, T.M. and Abbey, M.E. (2022) “Application of the Dupuit–Forchheimer model to groundwater flow into a well”. **Modeling Earth Systems and Environment,** 8:2359-2367, https://doi.org/10.1007/s40808-021-01224-2
44. Penny, G., Mullen, C., Bolster, D., Huber, B. and Muller, M.F. (2020) “anem: A Simple Web-Based Platform to Build Stakeholder Understanding of Groundwater Behavior”. **Groundwater,** 59(2):273-280, https://doi.org/10.1111/gwat.13043
45. Rodriguez-Pretelin, A. and Nowak, W. (2019) “Dynamic re-distribution of pumping rates in well fields to counter transient problems in groundwater production”. **Groundwater for Sustainable Development,** 8:606-616, https://doi.org/10.1016/j.gsd.2019.02.009

46. Samani, N. and Sedghi, M.M. (2015) “Semi-analytical solutions of groundwater flow in multi-zone (patchy) wedge-shaped aquifers”. **Advances in Water Resources,** 77: 1-16 https://doi.org/10.1016/j.advwatres.2015.01.003
47. Samani, N. and Zarei-Doudeji, S. (2012) “Capture zone of a multi-well system in confined and unconfined wedge-shaped aquifers”. **Advances in Water Resources,** 39: 71-84 https://doi.org/10.1016/j.advwatres.2012.01.004
48. Sedghi, M.M., Samani, N. and Sleep, B. (2012) “Boundary depletion rate and drawdown in leaky wedge-shaped aquifers”. **Hydrological Processes**, 26(20):3101-3113 https://doi.org/10.1002/hyp.8338
49. Sedghi, M.M., Samani, N. and Sleep, B. (2010) “Three-Dimensional Semianalytical Solutions of Groundwater Flow to a Well in Fractured Wedge-Shaped Aquifers”. **Journal of Hydrologic Engineering**, 15(12) https://doi.org/10.1061/(ASCE)HE.1943-5584.0000269
50. Sedghi, M.M. and Zhan, H. (2022) “On the discharge variation of a qanat in an alluvial fan aquifer”. **Journal of Hydrology**, 610:127922 https://doi.org/10.1016/j.jhydrol.2022.127922
51. Singh, S.K. (2001) “Identifying Impervious Boundary and Aquifer Parameters from Pump-Test Data”. **Journal of Hydrolic Engineering**, 127(4), https://doi.org/10.1061/(ASCE)0733-9429(2001)127:4(280)
52. Smerdon, B.D., Payton Gardner, W., Harrington, G.A. and Tickell, S.J. (2012) “Identifying the contribution of regional groundwater to the baseflow of a tropical river (Daly River, Australia”. **Journal of Hydrology**, 464-465:107-115, https://doi.org/10.1016/j.jhydrol.2012.06.058

53. Sun, J., Li, J., Liu, Q. and Zhang H. (2011) "Approximate Engineering Solution for Predicting Groundwater Table Variation During Reservoir Drawdown on the Basis of the Boussinesq Equation". **Journal of Hydrologic Engineering**, 16(10) https://doi.org/10.1061/(ASCE)HE.1943-5584.0000372

54. Teloglou, I.S. and Bansal, R.K. (2012) "Transient solution for stream–unconfined aquifer interaction due to time varying stream head and in the presence of leakage". **Journal of Hydrology**, 428-429:68-79, https://doi.org/10.1016/j.jhydrol.2012.01.024

55. Theim, G. (1906). Hydrologische methoden. Gebhardt, Leipzig, 56.

56. Wang, L., Dai, C. and Xue, L. (2018) "A Semi-analytical Model for Pumping Tests in Finite Heterogeneous Confined Aquifers With Arbitrarily Shaped Boundary". **Water Resources Research**, 54(4):3207-3216 https://doi.org/10.1002/2017WR022217

57. Winston, R.B. (2009) "ModelMuse-A graphical user interface for MODFLOW-2005 and PHAST" U.S. Geological Survey Techniques and Methods 6-A29, 52 p.

58. Winston, R.B. (2020) "ModelMuse version 4.3: U.S. Geological Survey Software Release, 16 August 2020". https://doi.org/10.5066/P9XMX92F

59. Yang, S.Y., Huang, C.S., Liu, C.H. and Yeh, H.D. (2014) "Approximate Solution for a Transient Hydraulic Head Distribution Induced by a Constant-Head Test at a Partially Penetrating Well in a Two-Zone Confined Aquifer". **Journal of Hydraulic Engineering**, 140(7) https://doi.org/10.1061/(ASCE)HY.1943-7900.0000884

60. Yeh, H.D. and Chang, Y.C. (2006) "New analytical solutions for groundwater flow in wedge-shaped aquifers with various topographic boundary conditions". **Advances in Water Resources**, 29(3):471-480 https://doi.org/10.1016/j.advwatres.2005.06.002

61. Yeh, H.D. and Chang, Y.C. and Zlotnik, V.A. (2008) "Stream depletion rate and volume from groundwater pumping in wedge-shape aquifers". **Journal of Hydrology**, 349(3-4):501-511 https://doi.org/10.1016/j.jhydrol.2007.11.025

62. Zipper, S.C., Gleeson, T., Kerr, B., Howard, J.K., Rohde, M.M., Carah, J. and Zimmerman, J. (2019) "Rapid and Accurate Estimates of Streamflow Depletion Caused by Groundwater Pumping Using Analytical Depletion Functions". **Water Resources Research**, 55(7):5807-5829 https://doi.org/10.1029/2018WR024403

63. Zlotnik, V.A., Kacimov, A. and Al-Maktoumi, A. (2017) "Estimating Groundwater Mounding in Sloping Aquifers for Managed Aquifer Recharge". **Groundwater**, 55(6):797-810 https://doi.org/10.1111/gwat.12530

64. Zlotnik, V.A., Toundykov, D. and Cardenas, M.B. (2015) "An Analytical Approach for Flow Analysis in Aquifers with Spatially Varying Top Boundary". **Groundwater**, 53(2):335-341 https://doi.org/10.1111/gwat.12205

Figure 1.

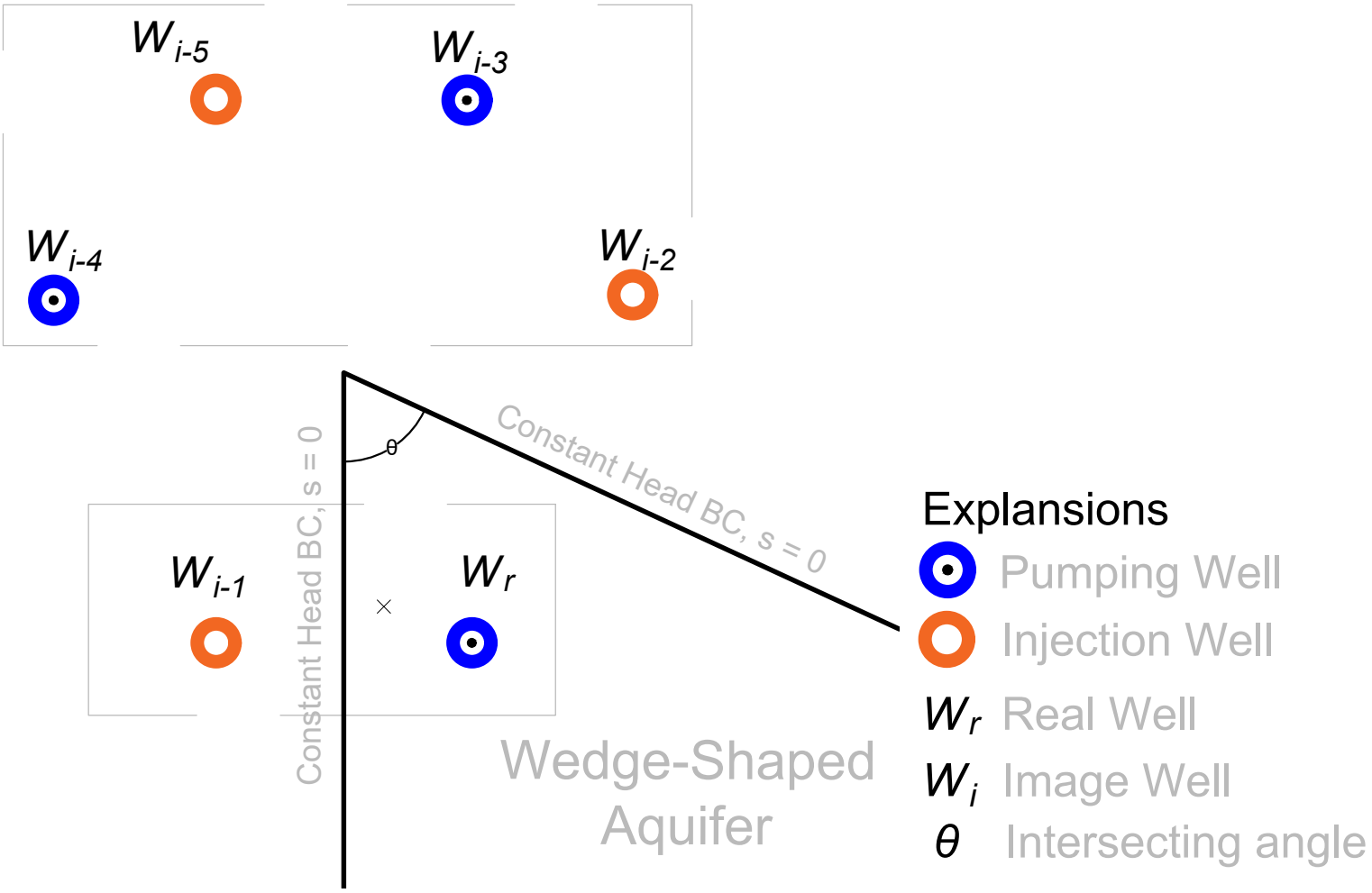
W_{i-5}
W_{i-3}
W_{i-4}
W_{i-2}
θ
Constant Head BC, s = 0
Constant Head BC, s = 0
W_{i-1}
W_r
Wedge-Shaped Aquifer
Explansions
Pumping Well
Injection Well
W_r Real Well
W_i Image Well
θ Intersecting angle

Figure 2.

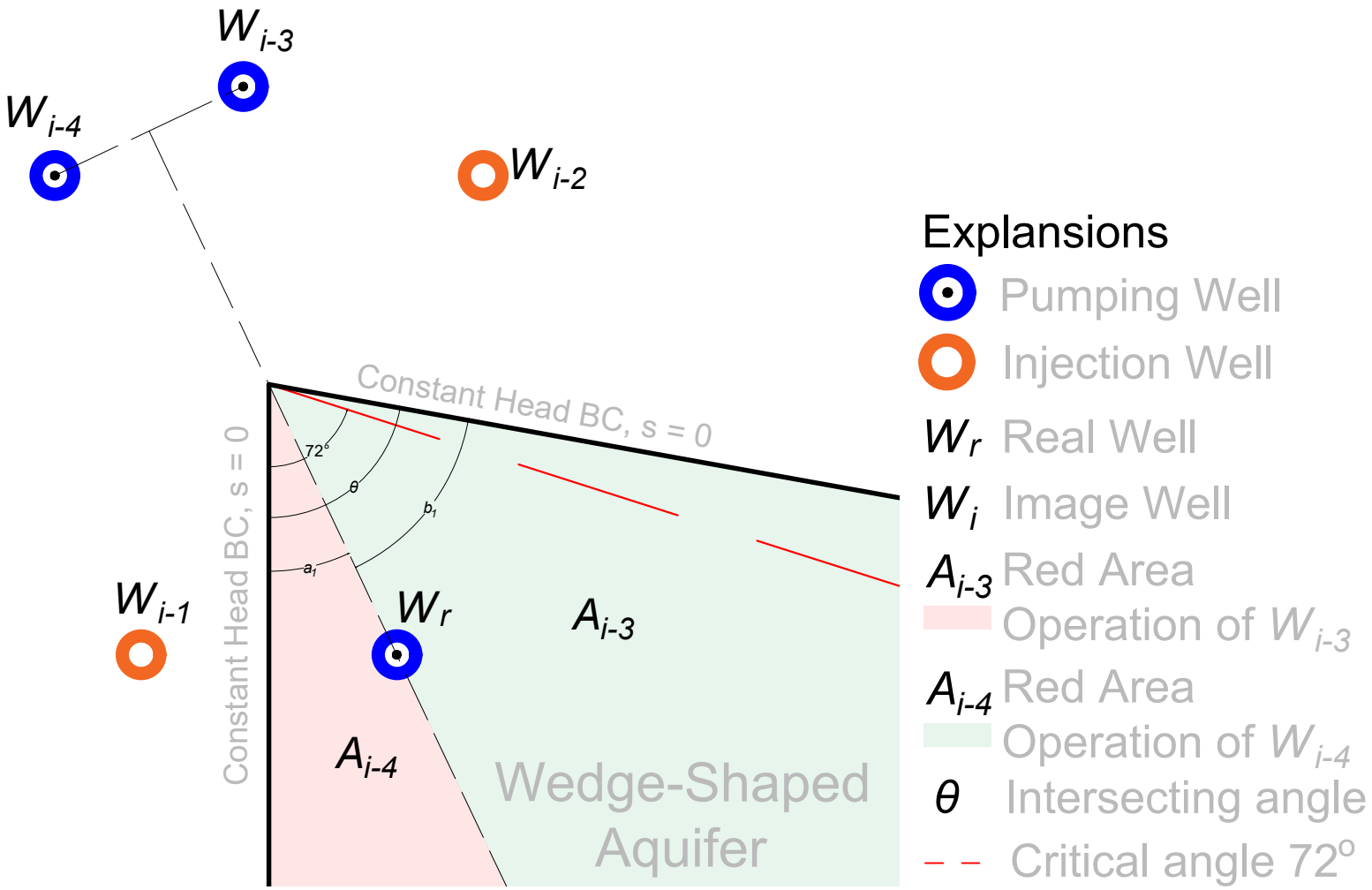
W_{i-3}
W_{i-4}
W_{i-2}
Constant Head BC, s = 0
Constant Head BC, s = 0
72°
θ
b_1
a_1
W_{i-1}
W_r
A_{i-3}
A_{i-4}
Wedge-Shaped Aquifer
Explansions
Pumping Well
Injection Well
W_r Real Well
W_i Image Well
A_{i-3} Red Area
Operation of W_{i-3}
A_{i-4} Red Area
Operation of W_{i-4}
θ Intersecting angle
Critical angle 72°

Figure 3.

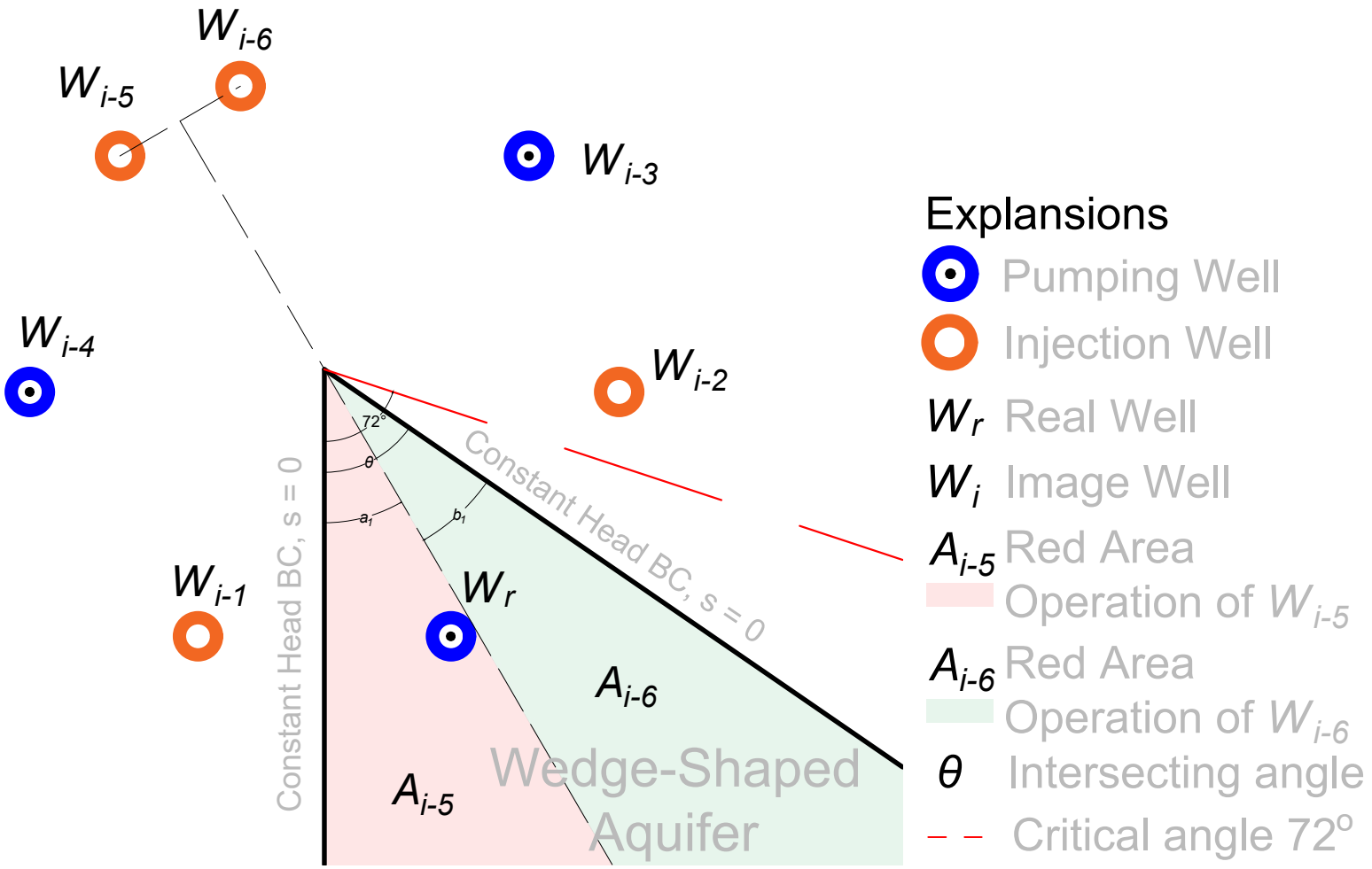
W_{i-6}
W_{i-5}
W_{i-3}
W_{i-4}
W_{i-2}
W_{i-1}
W_r
72°
θ
a_1
b_1
Constant Head BC, s = 0
Constant Head BC, s = 0
A_{i-6}
A_{i-5}
Wedge-Shaped Aquifer
Explansions
Pumping Well
Injection Well
W_r Real Well
W_i Image Well
A_{i-5} Red Area
Operation of W_{i-5}
A_{i-6} Red Area
Operation of W_{i-6}
θ Intersecting angle
Critical angle 72°

Figure 4.

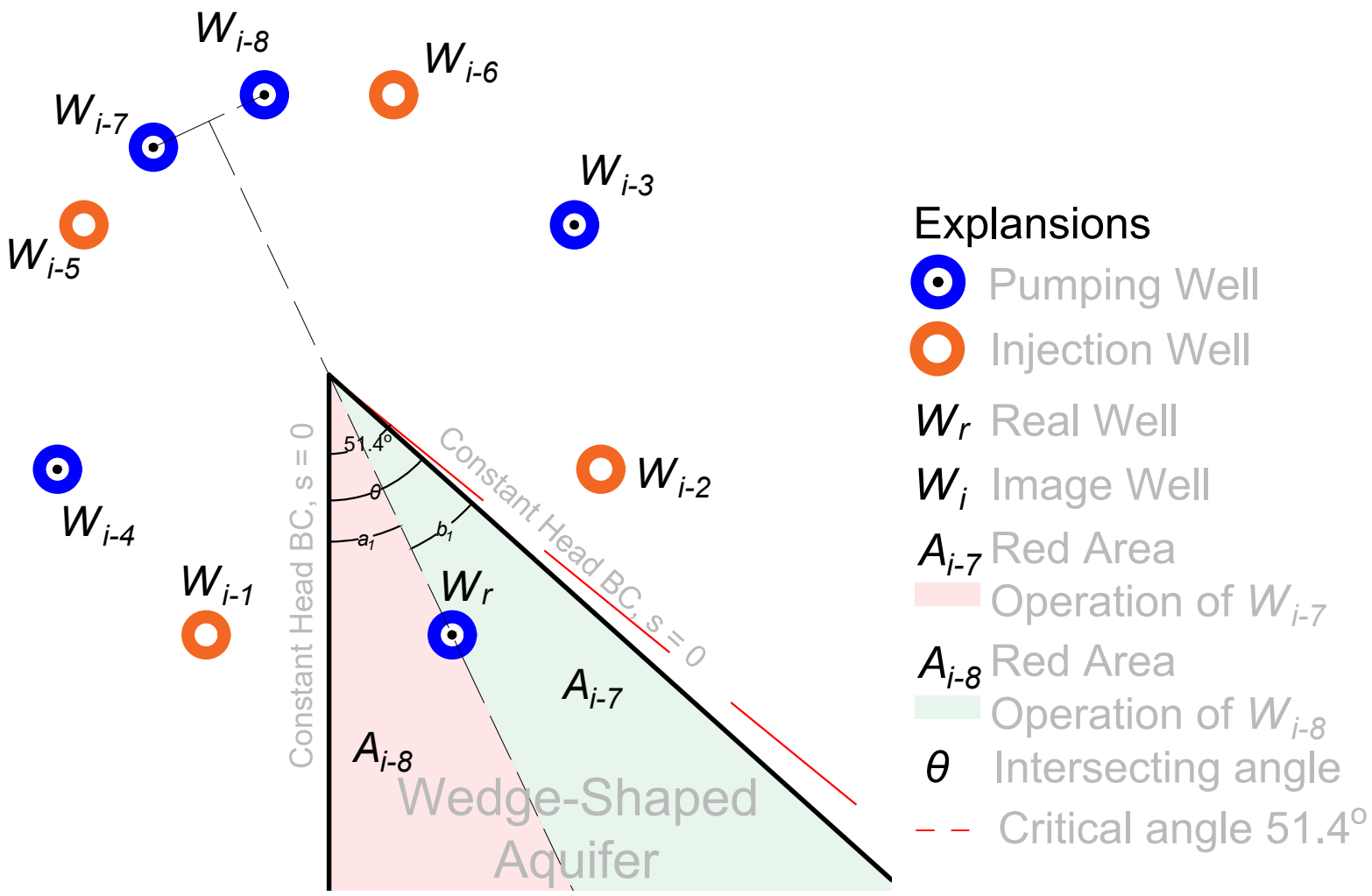
W_{i-8}
W_{i-6}
W_{i-7}
W_{i-3}
W_{i-5}
W_{i-2}
W_{i-4}
W_{i-1}
W_r
A_{i-7}
A_{i-8}
51.4°
θ
a_1
b_1
Constant Head BC, s = 0
Constant Head BC, s = 0
Wedge-Shaped Aquifer
Explansions
Pumping Well
Injection Well
W_r Real Well
W_i Image Well
A_{i-7} Red Area
Operation of W_{i-7}
A_{i-8} Red Area
Operation of W_{i-8}
θ Intersecting angle
Critical angle 51.4°

Figure 5.

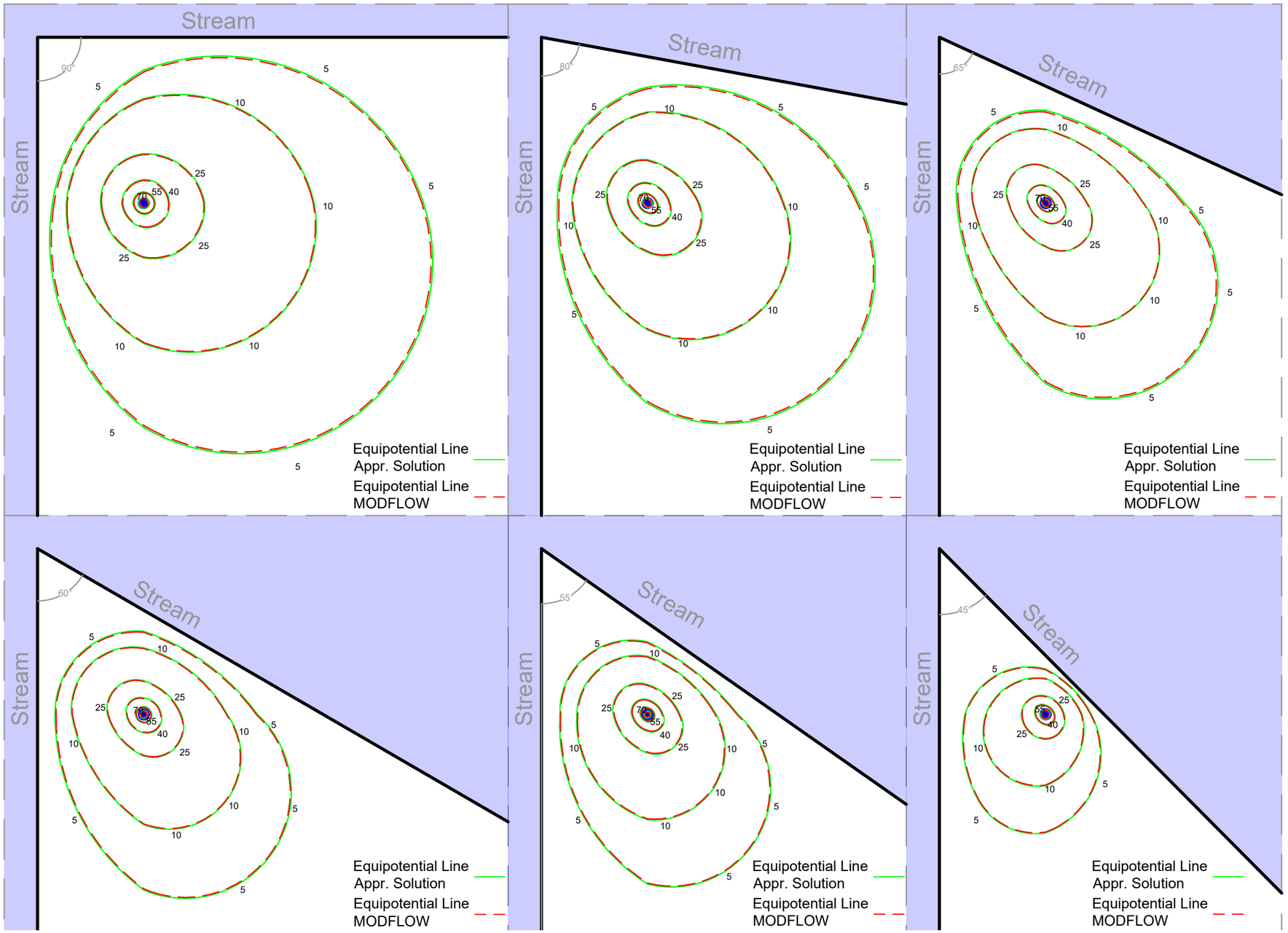
Stream
Stream
90°
5
10
25
40
55
70
85
Equipotential Line
Appr. Solution
Equipotential Line
MODFLOW
Stream
Stream
80°
Equipotential Line
Appr. Solution
Equipotential Line
MODFLOW
Stream
Stream
65°
Equipotential Line
Appr. Solution
Equipotential Line
MODFLOW
Stream
Stream
60°
Equipotential Line
Appr. Solution
Equipotential Line
MODFLOW
Stream
Stream
55°
Equipotential Line
Appr. Solution
Equipotential Line
MODFLOW
Stream
Stream
45°
Equipotential Line
Appr. Solution
Equipotential Line
MODFLOW

Figure 6.

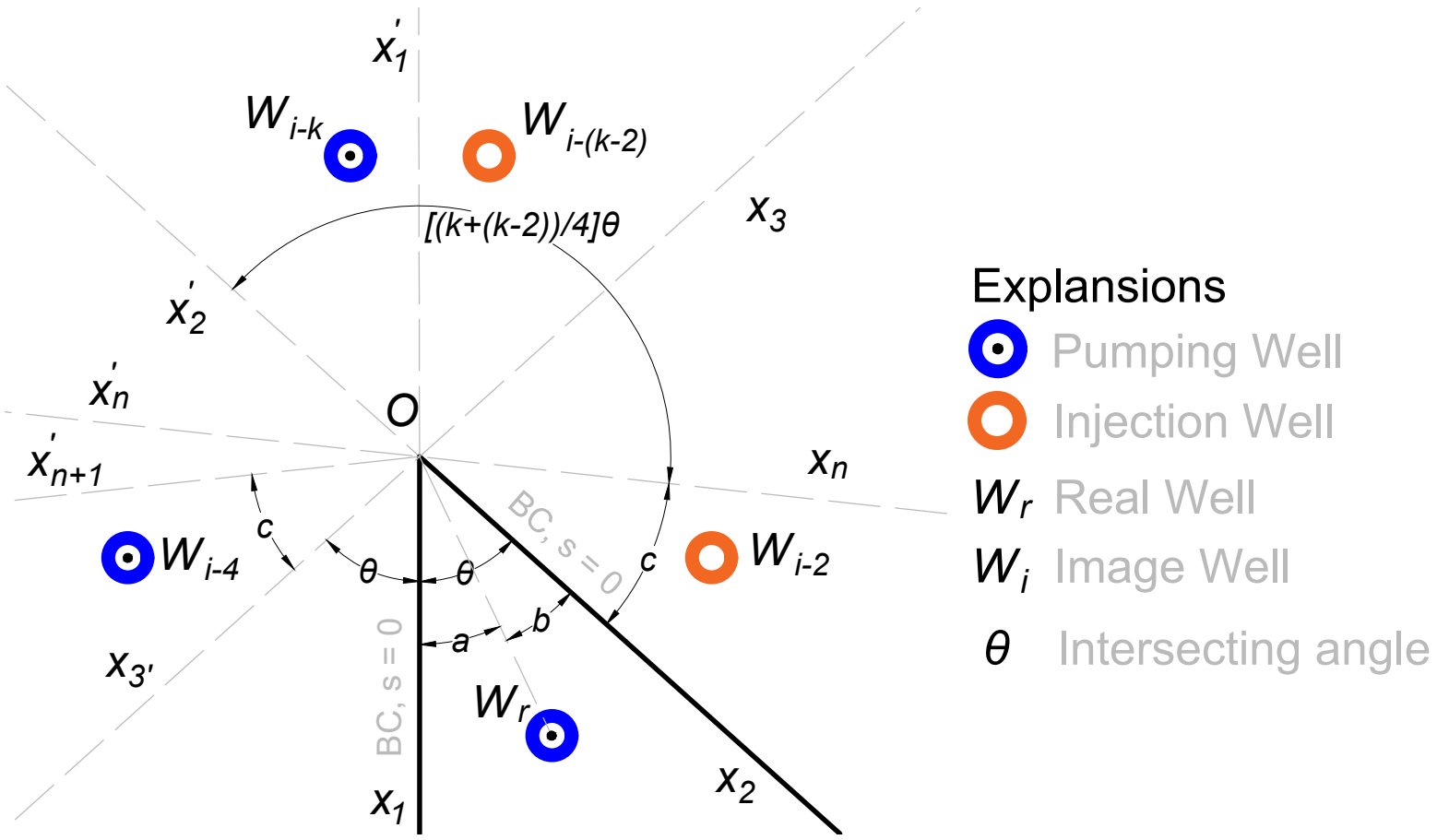
x_1'
W_{i-k}
$W_{i-(k-2)}$
x_3
$[(k+(k-2))/4]\theta$
x_2'
x_n'
O
x_{n+1}'
x_n
c
W_{i-4}
θ
θ
BC, s = 0
c
W_{i-2}
a
b
$x_{3'}$
BC, s = 0
W_r
x_1
x_2
Explansions
Pumping Well
Injection Well
W_r Real Well
W_i Image Well
θ Intersecting angle